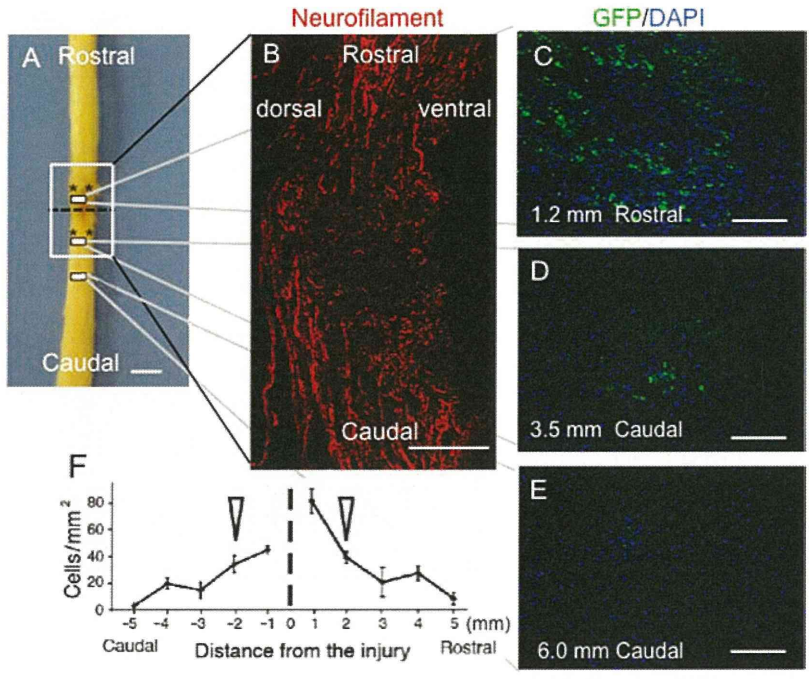

Figure 3. Transplanted bone marrow-derived neural progenitor cells (BM-NPCs) in the injured spinal cord 8 weeks after transection. (A) Schematic drawing of a representative spinal cord from the BM-NPC group showing sites of transection (dotted line) and transplantation (*). (B) Representative longitudinal section stained for neurofilaments corresponding to the white box in (A), showing anatomical continuity of spinal cord parenchyma at the injury site. (C–E) Distribution of green fluorescent protein (GFP)-positive transplanted cells at sites 1.2 mm rostral (C), 3.5 mm caudal (D), and 6.0 mm caudal (E) to the injury center in the dorsal spinal cord. Positions of the panels are indicated by small boxes in (A). (F) Numbers of GFP-positive cells between 5 mm caudal and 5 mm rostral to the injury center. The dotted line and arrowheads indicate the transected portion and the site of cell transplantation, respectively. Note that the GFP-positive cells were incorporated into the host spinal cord. DAPI, 4′,6-diamidino-2-phenylindole. Scale bars: 2 mm (A), 250 μm (B), 100 μm (C–E).

Fluorogold Tracing Detected Extension of Neurites From BM-NPCs Across the Transected Site in the Spinal Cord

Four days before the animals were sacrificed, we injected the retrograde tracer FG 10 mm caudal to the transected site, so that FG would be taken up through the terminals of the regenerated neurites (Fig. 7A). Strikingly, in the BM-NPC group, we detected FG-labeled grafted cells in the rostral as well as caudal spinal cord in all four rats (Fig. 7B–G). The presence of cells double positive for FG and GFP rostral to the transected portion indicated that the grafted cells extended their neurites across the transected portion to reach the caudal spinal cord. The site of injection was carefully examined to ensure that no FG could have reached the transected portion by diffusion (24). The number of cells labeled with FG and GFP at the rostral boundary of the transected spinal cord was $5.17 \pm 0.75/mm^2$ in the BM-NPC group. FG-labeled BM-NPCs were located rostrally 1.8 ± 0.18 mm from the transection stump to a maximum of 4.6 mm. In the vehicle group, no FG-labeled cells were found in the spinal cord rostral to the transected site. In any of the injured animals with or without treatments ($n = 4$, each group), no FG-labeled cells were found in the cervical spinal cord or in the brain sections.

Behavioral Analysis Indicated Improved Hind Limb Locomotor Function After BM-NPC Transplantation

BBB locomotor scores for the BM-NPC and vehicle groups were determined each week for 8 weeks after injury (Fig. 8). Improvements in hind limb motor function were significantly greater in the BM-NPC group than in the vehicle group after 2 weeks ($p < 0.01$) and over 3–8 weeks ($p < 0.001$, repeated measures ANOVA followed by post hoc Tukey's test). Mann–Whitney U test also indicated significant functional recovery between 2 and 8 weeks (Fig. 8). Eight weeks after the injury, averaged BBB scale of injured animals was 3.31 in the control group while 5.80 in BM-NPCs transplantation group. Following the treatments, rats showed symptoms of recovery; they showed extensive movements of the three joints in the hind limbs. The difference between these groups was statistically significant ($p < 0.001$, post hoc Tukey's test; $p < 0.01$, Mann–Whitney U test).

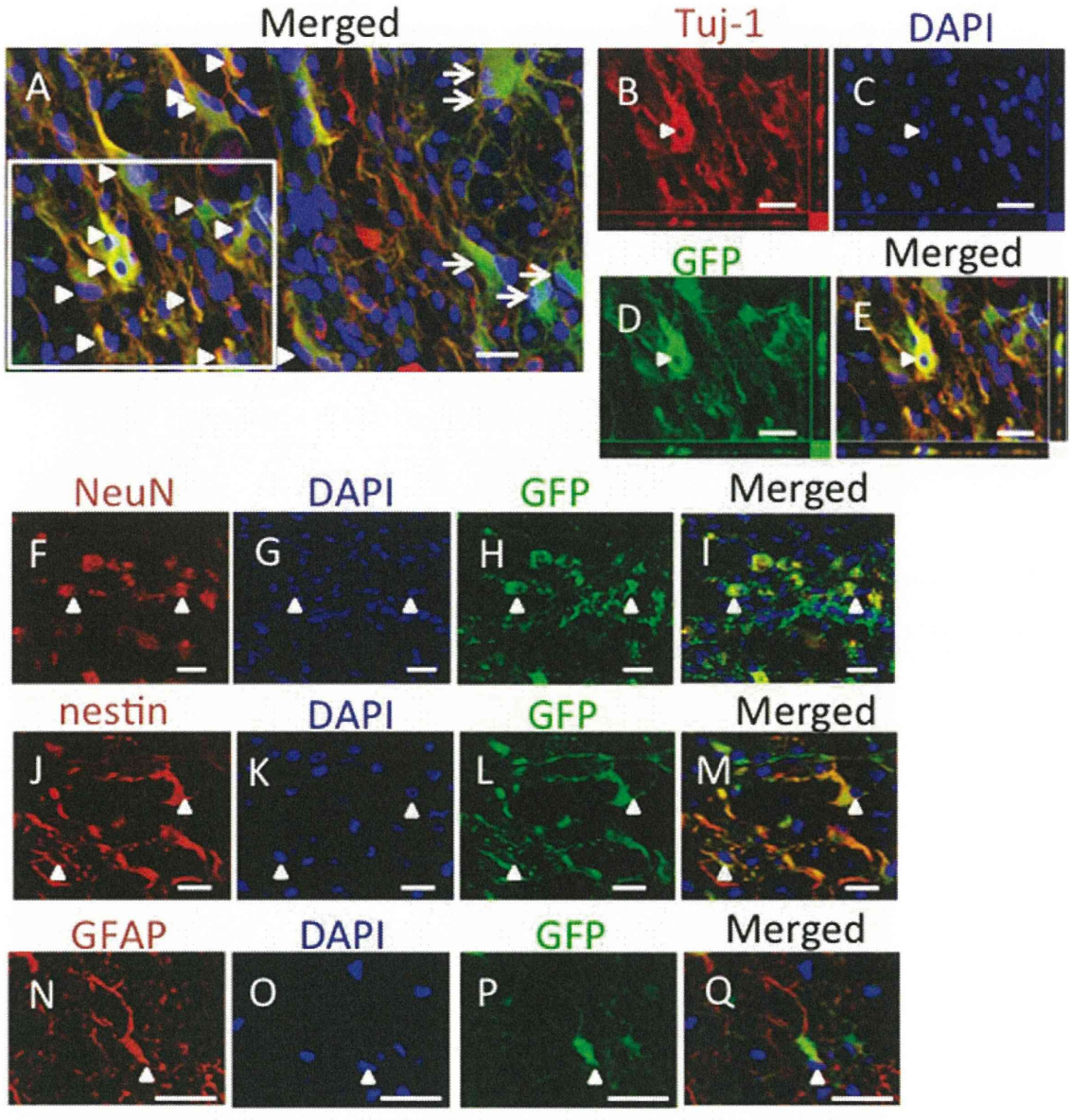

Figure 4. Differentiation of green fluorescent protein (GFP)-positive bone marrow-derived neural progenitor cells (BM-NPCs) in the spinal cord 8 weeks after injury. (A–Q) Cells labeled with neuron-specific class III β-tubulin (antibody: Tuj-1) (A–E) and neuronal nuclei (NeuN) (F–I) were encountered more frequently than those labeled with nestin (J–M) or glial fibrillary acidic protein (GFAP) (N–Q). Arrowheads, positively labeled cells. Arrows, GFP-positive and Tuj-1-negative cells. DAPI, 4′,6-diamidino-2-phenylindole. Scale bars: 20 μm.

Functional MRI Was Not Able to Provide Evidence of Reconstruction of Local Neuronal Networks After BM-NPC Transplantation

In response to electrical stimulation to the hind limbs, we counted fMRI signals in the bilateral somatosensory cortex in both BM-NPC and vehicle groups. BOLD signal changes were as high as 2.4% in the original hind limb territory in the BM-NPC group (Fig. 9). In the contralateral hind limb territory (HL) as defined in Figure 9B (36), volumes of activation in the BM-NPC group were significantly larger than those in the vehicle group ($p = 0.014$, Student's t test) (Fig. 9C). Particularly, we noticed that cortical activation in spinally injured rats was not confined to the original hind limb territory in the primary somatosensory cortex (Fig. 9D). Signals extended more medially and even to the ipsilateral side of stimulation. Total volumes of cortical activation were 1.53 ± 0.83 and 0.41 ± 0.17 mm^3 in the BM-NPC and vehicle groups, respectively, while the difference was not statistically significant ($p = 0.11$, Student's t test).

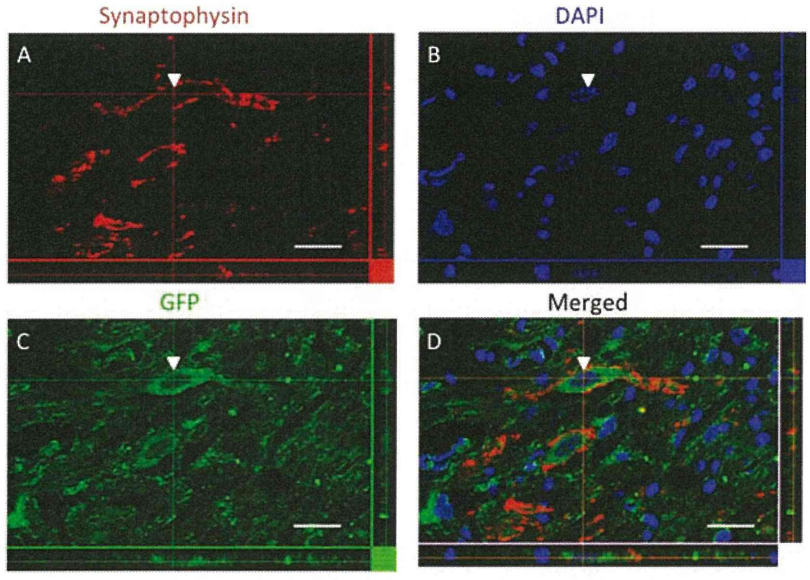

Figure 5. Synaptophysin expressed around GFP-positive bone marrow-derived neural progenitor cells (BM-NPCs). Photomicrographs depicting synaptophysin (A), DAPI (B), GFP (C), and a merged image (D) staining of transplanted cells in the spinal cord. This finding suggests the synapse formation between the transplanted cells and host cells. Arrowheads indicate positively labeled cells. Abbreviations are as in Figure 4. Scale bars: 20 μm.

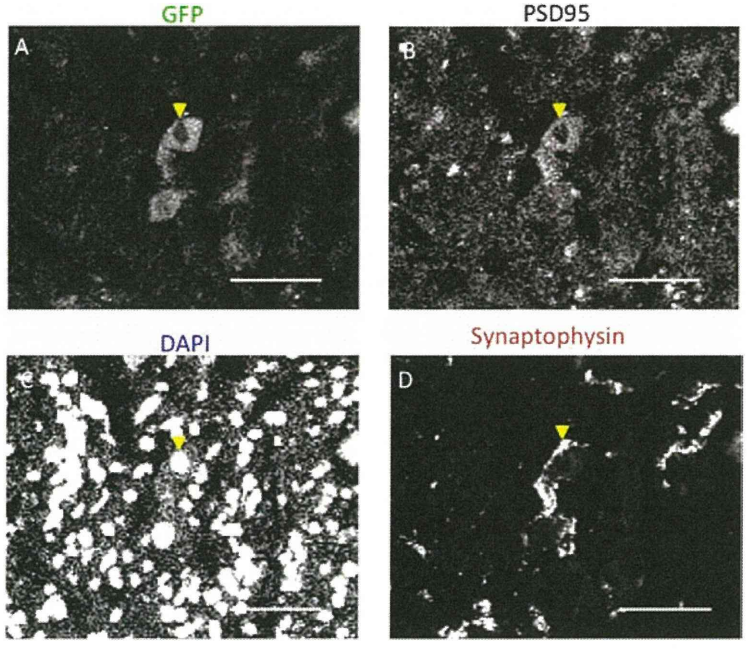

Figure 6. Postsynaptic density (PSD-95) localized adjacent to synaptophysin on GFP-positive bone marrow-derived neural progenitor cells (BM-NPCs). Photomicrographs depicting GFP (A), PSD-95 (B), DAPI (C), and synatophysin (D) staining of cells in the spinal cord. This finding suggests synapse formation between the transplanted cells and host cells. Arrowheads indicate positively labeled cells. Abbreviations are as in Figure 4. Scale bars: 50 μm.

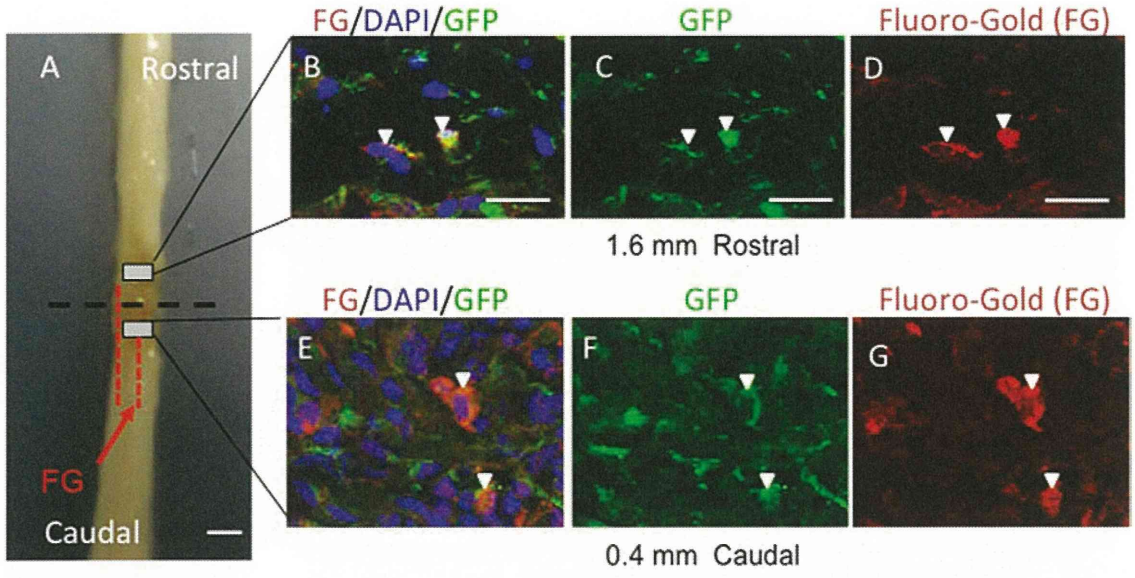

Figure 7. Expression of the retrograde tracer Fluorogold (FG) injected 10 mm caudal to the transected site of the spinal cord. (A) Schematic drawing of a representative spinal cord taken from the bone marrow-derived neural progenitor cell (BM-NPC) group, showing sites of FG injection (red arrow). Red dotted lines indicate the supposed routes by which FG was transported from the terminals of extended neurites and crossed the transected portion. (B–G) Green fluorescent protein (GFP)-positive BM-NPCs, transplanted rostral (B–D) and caudal (E–G) to the injured site, were also positive for FG in representative sections obtained 1.6 mm rostral and 0.4 mm caudal to the transected site. Abbreviations, schematic drawings, and arrowheads are as described in Figures 2 and 3. Scale bars: 2.0 mm (A) and 20 μm (B–G).

DISCUSSION

In this study, we report that transplantation of BM-NPCs promoted functional recovery of the spinally injured animals evidenced by improved locomotor scores. The grafted cells survived and committed predominant neuronal differentiation in the injured spinal cord. Immunohistochemistry using synaptophysin and PSD-95 as well as the FG tracing indicated synaptic formation of the BM-NPCs with the surrounding neurons and extension of the neurites across the transected portion in the spinal cord. As a consequence, neuronal networks were partially restored 7 weeks posttransplantation, which was represented as increased cortical signals in fMRI of the BM-NPC transplanted animals. However, the representation of the cortical signals was diverse and altered when compared to the original sensory map. Therefore, reestablishment of neuronal networks by transplantation of BM-NPCs was not fully accomplished.

Here, we demonstrated that transplantation of BM-NPCs was an efficient method in supplying neuronal lineage cells in a severely injured spinal cord. Majority of sphere-derived cells cultured with several trophic factors were reported to express neuronal markers such as βIII tubulin (Tuj-1) and microtubule associated protein 2 in a high ratio

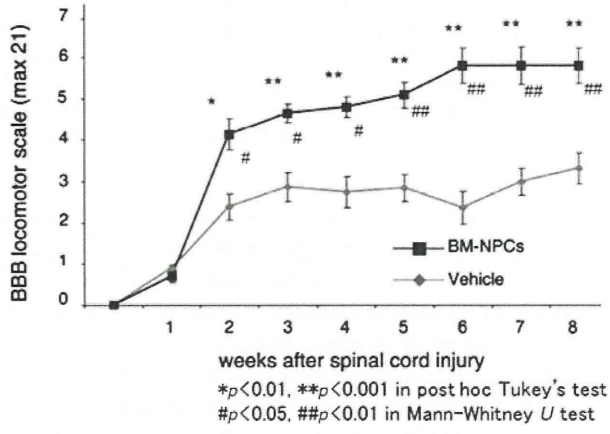

Figure 8. Basso, Beattie, Bresnahan (BBB) locomotor scale. Open-field locomotor hind limb function of all rats was tested on the day after injury and then weekly for 8 weeks postoperatively. Results are shown separately for groups transplanted on day 9 with bone marrow-derived neural progenitor cells (BM-NPCs) ($n=10$) or injected with vehicle ($n=14$). Repeated measures ANOVA followed by the post hoc Tukey's test as well as Mann–Whitney U test showed significant differences between the groups. Two weeks after injury, BBB scores of the BM-NPC group were significantly higher than those of the vehicle group. $*p<0.01$, $**p<0.001$ post hoc Tukey's test. $\#p<0.05$, $\#\#p<0.01$ Mann–Whitney U test.

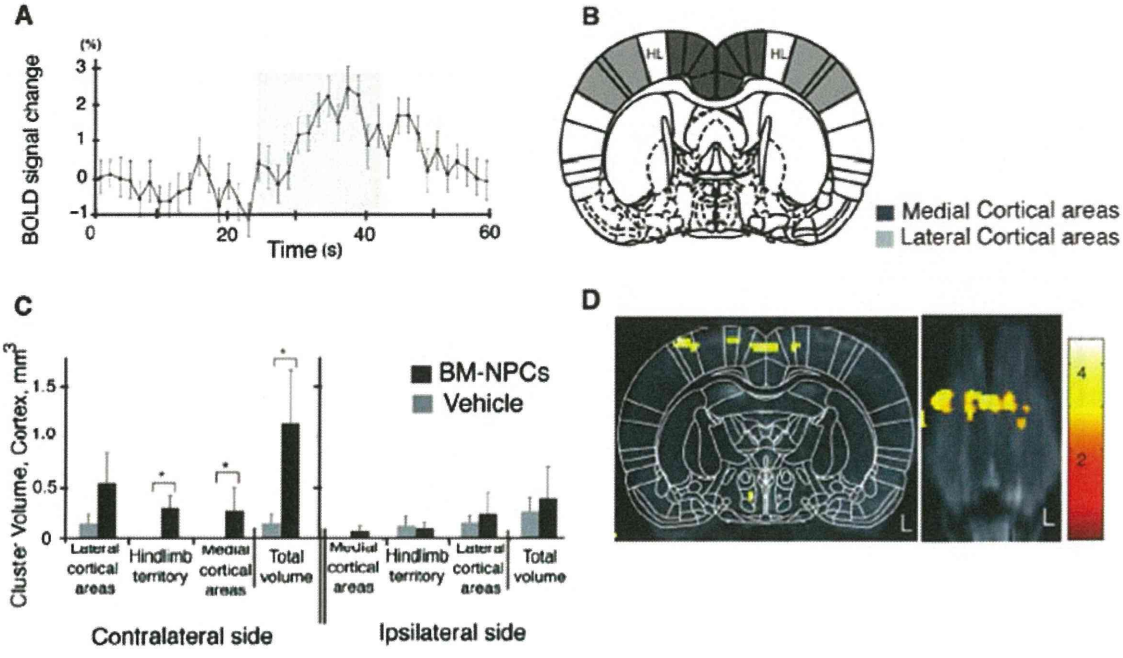

Figure 9. Cortical fMRI signals in response to hind limb stimulation 8 weeks after spinal cord transection. (A) Time course of blood oxygenation level-dependent (BOLD) signals (%) in a voxel in the original hind limb territory in the bone marrow-derived neural progenitor cell (BM-NPC) transplantation group ($n=6$). Gray bars indicate the period of stimulation. (B) Schematic drawing of a rat brain to illustrate medial cortical areas (dark gray), the hind limb territory of the primary somatosensory cortex area (HL) and lateral cortical areas (light gray), in which cortical activations were counted. (C) Volumes of functional magnetic resonance imaging (fMRI) signals in vehicle and BM-NPC groups. Significant differences between the BM-NPC and vehicle injection groups were noted in the signals in the contralateral cortex and the hind limb territory of the contralateral side to the stimulation ($*p<0.05$). Note that broad cortical areas were activated in response to hind limb stimulation 8 weeks after spinal cord injury. (D) A representative cortical sensory map from the BM-NPCs group, demonstrating neuronal activation in various cortical areas outside of the original hind limb territory in the primary somatosensory cortex. Signals were observed on the left side (L), which was ipsilateral to the stimulation as demonstrated in a coronal section (left) at bregma −1.4 mm and a horizontal section (right). The color scale indicates T statistics calculated by statistical parametric mapping software (SPM2). The coronal sections are superimposed on a schematic brain section from the same level [reproduced with permission of Elsevier from the Paxinos and Watson atlas (36)].

(98.5% and 95.7%, respectively) and GFAP in a low ratio (0.7%) (17). These findings clearly indicated that cells in the BM-NPC-derived spheres tended to differentiate into neurons and were not initially committed to the glial fate. In the same study in which BM-NPC-derived spheres were transplanted into the rat stroke model, BM-NPCs predominantly differentiated into NeuN-expressing postmitotic neurons (79.5%), and only a small population of the transplanted cells expressed GFAP (1.9%) (17). In the present study, we found that the rate of the differentiation of the transplanted GFP-positive cells into the neuronal fate detected by Tuj-1-positive cells was 77.2%; however, that of postmitotic neurons positive for NeuN was only 36.0%. The rate of differentiation into GFAP-positive astrocytes was 2.9%, similar to that observed in the transplantation into the rat stroke model. These observations indicate that, although the ratio of the differentiation into postmitotic neurons was dependent on the disease models, the BM-NPC-derived sphere cells predominantly differentiate into the neuronal fate after transplantation.

In general, the environment of the spinal cord is not permissive for survival and neuronal differentiation of the transplanted cells (19,27). Exogenous neural stem cells undergo proliferation and differentiate mainly into astrocytes in the spinal cord (33). When naive neural stem cells were transplanted into the injured spinal cord, 84% of the cells were GFAP-positive 9 weeks after transplantation, while only 4% of the cells had neuronal characteristics (18). Even when cells are shown to differentiate into neuronal lineage cells in vitro, the degree of neural induction in vivo may turn out to be less than expected after transplantation into the injured spinal cord (7). Our findings indicate that BM-NPCs are a reliable source of neuronal cells that can be used in cell transplantation therapy for SCI. Previously, we transplanted BM-NPCs and naive BMSCs in a rat stroke model and compared the results (17), in which BM-NPCs demonstrated much higher efficacy in survival, differentiation, and integration into the host brain. Having established the difference between BM-NPCs and naive BMSCs, we solely used BM-NPCs in the current protocol.

As Abematsu et al. demonstrated recently, grafted neuronal cells may establish neuronal connectivity by making synaptic connections with endogenous surrounding neurons (1). In this study, immunohistochemistry for synaptophysin and PSD-95 revealed the adjacent localization of synaptophysin and PSD-95 in the same GFP-positive transplanted cells (Fig. 6). Synaptophysin and PSD-95 are markers for presynaptic vesicles and postsynaptic density, respectively, suggesting that the transplanted cells constructed synaptic connections and received synaptic inputs from host and/or surrounding neurons.

In our model, retrograde axonal tracing showed the presence of cells double positive for FG and GFP in the spinal cord rostral to the transected portion. However, no FG-positive cells were detected in cervical spinal cord or brain sections, when we performed histological analyses 4 days following the injection of FG. In a previous report using a matrix seeded with BMSCs to fill the gap of the spinal cord transection injury, FG-labeled neurons were detected in the cortex and in the brainstem a week after the FG injection (22). With regard to the time between the FG injections and histological analyses, 4 days might not be long enough for the retrograde tracers to reach the brain stem through the severely injured spinal cord. Therefore, the purpose of the FG tracing was focused on evaluating grafted BM-NPCs located rostral to the transected stump. To avoid confusion in interpreting results, we only injected FG caudally and 10 mm from the stump. In this way, we could minimize the possibility that the tracer would diffuse and go across the transected portion (22). Results of the FG thus indicated that the grafted cells survived, differentiated, and might have extended neurites across the transected portion of the spinal cord.

Furthermore, the FG-labeled BM-NPCs localized 4.6 mm rostral to the spinal cord stump. Recently, we demonstrated the capacity of migration of BM-NPCs in a rat model of stroke (17). In spinal cord, various studies using in vivo MRI tracking systems have observed that the transplanted cells could actually migrate long distances. In one of these study, injected live cells traveled as far as 9 mm in 8 weeks following the transplantation (23). Although it is possible that dispersion might have transferred the grafted cells a few millimeters, the aforementioned information suggested that the BM-NPCs had the capacity to migrate in the spinal cord.

In this study, transplantation of BM-NPCs to the completely transected adult rat spinal cord led to a significant, albeit modest improvement of hind limb motor function as determined by BBB scoring. Eight weeks after the injury, the BBB score of injured animals was 3.3 without BM-NPC transplantation, while with the transplantation, it improved to 5.8. In other studies, BMSC-derived Schwann cells or olfactory mucosa were transplanted into similar complete spinal cord transection models in Wistar rats. In those studies, BBB scores were 3.6 and 2.6 in the controls, while 7.0 and 4.6 in the treatment groups, respectively (3,20). Degrees of improvement in BBB scores by BM-NPC transplantations were therefore comparable to those of the other studies. Importantly, to judge degrees of locomotor recovery by the BBB scores needs caution, since functional improvement may also depend on the strains used or the types of treatments applied. For instance, in Sprague–Dawley strains, BBB scores were lower and between 0 and 2 following complete transection of the spinal cord (13,26,41). In one of these studies, 10 weeks posttransplantation of olfactory ensheathing cells, BBB scores improved to 4.3 from 1.0 (26).

FMRI also demonstrated an increase of BOLD signals in cortex cerebri in response to electrical stimulation of a hind limb. In particular, cortical activations were not only observed in the original somatosensory cortex, rather the BOLD signals had an abnormal and diverse distribution, including ipsilateral activity. Together, the addition of the BM-NPCs to the injury area might lead to the reestablishment of a degree of ascending and descending neurotransmission across injury, while we could not confirm reconstruction of the disrupted neuronal networks by the distribution of recovered cortical activations in fMRI.

One of the reasons for such ambiguity could partly rely on the end point of this study, which was 7 weeks posttransplantation. In the current methods, we set the end point mainly based on the time course of locomotor recovery. As shown in Figure 8, BBB scores improved and reached a plateau 5–6 weeks after the transplantation. In another experiment using fMRI to evaluate sensory recovery in a rat model of SCI, fMRI was performed 9 weeks posttransplantation, which demonstrated recovery of cortical responses (18). Moreover, in our previous experiment applying BMSC-derived Schwann cells to a rat model of complete spinal cord transection, it was 6 weeks posttransplantation when the axonal regeneration was histologically confirmed (20). However, as we demonstrated previously, reorganization in cerebral cortex may take place over 6 months long after SCI (13). After severe thoracic SCI, cortical connections from the spared forelimbs expanded and took over the deafferented hind limb areas (13,16). If such deafferentation plasticity occurs, the corresponding somatosensory cortex may no longer be available to receive or process recovered ascending sensory information. In this sense, the time allowed for recovery following the complete transection could be too short and limit the value of fMRI in this study.

Another possible explanation for the diverse cortical signals in fMRI is misdirection of sensory inputs through the reconstructed neuronal networks. After transplantation of BM-NPCs, new synaptic pathways relaying peripheral inputs to cortical areas were formed in the injured spinal cord. However, they could be different from those in the original ascending tracts. In such a situation, recovered

sensory inputs would not connect with the original hind limb territory, but with various cortical areas.

Besides specific neuronal cell induction, another possible strategy for treating SCI includes transduction of neural stem cells into the oligodendrocytic lineage to enhance myelination (18,21). Using this approach, myelination of spared axons led to recovery of conduction velocity and promoted functional recovery in SCI. Hypothetically, however, if axons are completely severed in the damaged spinal cord, as occurs in our injury model and a model used by others (1), enhancement of myelination with oligodendrocytes may have limited effectiveness. In this situation, a strategy in which added neuronal cells may serve as a form of interneuron providing a link across the injury may be a more reliable approach. Depending on the degree of injury, one may need to select or combine different types of cell transplantation to achieve the best functional recovery.

We conclude that delayed grafting of BM-NPCs into the injured spinal cord was effective in providing neuronal lineage cells. If an efficient neuronal induction in the injured spinal cord was feasible, reconstruction of disrupted neuronal circuits between grafted cells and endogenous surrounding neurons can be a possible means of achieving recovery from SCI. Depending on the degrees of SCI, we can select or combine different types of cell transplantation to achieve the best functional recovery in SCI and other neural degenerative diseases occurring in the spinal cord.

ACKNOWLEDGMENTS: We thank Ms. Ryoko Mamiya for her technical assistance and Dr. Mitsunobu Matsubara and Dr. Kuniyasu Niizuma (Tohoku University) for their useful inputs to our project. This work was supported by Program for Promotion of Fundamental Studies in Health Sciences of the National Institute of Biomedical Innovation (NIBIO). This work was supported by Program for Promotion of Fundamental Studies in Health Sciences of the National Institute of Biomedical Innovation (NIBIO). The authors declare no conflict of interest.

REFERENCES

1. Abematsu, M.; Tsujimura, K.; Yamano, M.; Saito, M.; Kohno, K.; Kohyama, J.; Namihira, M.; Komiya, S.; Nakashima, K. Neurons derived from transplanted neural stem cells restore disrupted neuronal circuitry in a mouse model of spinal cord injury. J. Clin. Invest. 120:3255–3266; 2010.
2. Ankeny, D. P.; McTigue, D. M.; Jakeman, L. B. Bone marrow transplants provide tisssue protection and directional guidance for axons after contusive spinal cord injury in rats. Exp. Neurol. 190:17–31; 2004.
3. Aoki, M.; Kishima, H.; Yoshimura, K.; Ishihara, M.; Ueno, M.; Hata, K.; Yamashita, T.; Iwatsuki, K.; Yoshimine, T. Limited functional recovery in rats with complete spinal cord injury after transplantation of whole-layer olfactory mucosa: Laboratory investigation. J. Neurosurg. Spine 12: 122–130; 2010.
4. Azizi, S. A.; Stokes, D.; Augelli, B. J.; DiGirolamo, C.; Prockop, D. J. Engraftment and migration of human bone marrow stromal cells implanted in the brains of albino rats—similarities to astrocyte grafts. Proc. Natl. Acad. Sci. USA 95(7):3908–3913; 1998.
5. Baptiste, D. C.; Fehlings, M. G. Update on the treatment of spinal cord injury. Prog. Brain Res. 161:217–233; 2007.
6. Basso, D. M.; Beattie, M. S.; Bresnahan, J. C. A sensitive and reliable locomotor rating scale for open field testing in rats. J. Neurotrauma 12:1–21; 1995.
7. Cao, Q. L.; Howard, R. M.; Dennison, J. B.; Whittemore, S. R. Differentiation of engrafted neuronal-restricted precursor cells is inhibited in the traumatically injured spinal cord. Exp. Neurol. 177:349–359; 2002.
8. Cheng, C.; Gao, S.; Zhao, J.; Niu, S.; Chen, M.; Li, X.; Qin, J.; Shi, S.; Guo, Z.; Shen, A. Spatiotemporal patterns of postsynaptic density (PSD)-95 expression after rat spinal cord injury. Neuropathol. Appl. Neurobiol. 34:340–356; 2007.
9. Dezawa, M.; Hoshino, M.; Nabeshima, Y.; Ide, C. Marrow stromal cells: Implications in health and disease in the nervous system. Curr. Mol. Med. 5:723–732; 2005.
10. Dezawa, M.; Kanno, H.; Hoshino, M.; Cho, H.; Matsumoto, N.; Itokazu, Y.; Tajima, N.; Yamada, H.; Sawada, H.; Ishikawa, H.; Mimura, T.; Kitada, M.; Suzuki, Y.; Ide, C. Specific induction of neuronal cells from bone marrow stromal cells and application for autologous transplantation. J. Clin. Invest. 113:1701–1710; 2004.
11. Ding, D. C.; Shyu, W. C.; Lin, S. Z. Mesenchymal stem cells. Cell Transplant. 20:5–14; 2011.
12. Endo, T.; Spenger, C.; Hao, J.; Tominaga, T.; Wiesenfeld-Hallin, Z.; Olson, L.; Xu, X. J. Functional MRI of the brain detects neuropathic pain in experimental spinal cord injury. Pain 138:292–300; 2008.
13. Endo, T.; Spenger, C.; Tominaga, T.; Brene, S.; Olson, L. Cortical sensory map rearrangement after spinal cord injury: fMRI responses linked to Nogo signalling. Brain 130:2951–2961; 2007.
14. Filbin, M. T. Myelin-associated inhibitors of axonal regeneration in the adult mammalian CNS. Nat. Rev. Neurosci. 4:703–713; 2003.
15. Fitch, M. T.; Silver, J. CNS injury, glial scars, and inflammation: Inhibitory extracellular matrices and regeneration failure. Exp. Neurol. 209:294–301; 2008.
16. Ghosh, A.; Haiss, F.; Sydekum, E.; Schneider, R.; Gullo, M.; Wyss, M. T.; Mueggler, T.; Baltes, C.; Rudin, M.; Weber, B.; Schwab, M. E. Rewiring of hindlimb corticospinal neurons after spinal cord injury. Nat. Neurosci. 13:97–104; 2010.
17. Hayase, M.; Kitada, M.; Wakao, S.; Itokazu, Y.; Nozaki, K.; Hashimoto, N.; Takagi, Y.; Dezawa, M. Committed neural progenitor cells derived from genetically modified bone marrow stromal cells ameliorate deficits in a rat model of stroke. J. Cereb. Blood Flow Metab. 29:1409–1420; 2009.
18. Hofstetter, C. P.; Holmstrom, N. A.; Lilja, J. A.; Schweinhardt, P.; Hao, J.; Spenger, C.; Wiesenfeld-Hallin, Z.; Kurpad, S. N.; Frisen, J.; Olson, L. Allodynia limits the usefulness of intraspinal neural stem cell grafts; directed differentiation improves outcome. Nat. Neurosci. 8:346–353; 2005.
19. Johnson, P. J.; Tatara, A.; Shiu, A.; Sakiyama-Elbert, S. E. Controlled release of neurotrophin-3 and platelet-derived growth factor from fibrin scaffolds containing neural progenitor cells enhances survival and differentiation into neurons in a subacute model of SCI. Cell Transplant. 19: 89–101; 2010.
20. Kamada, T.; Koda, M.; Dezawa, M.; Yoshinaga, K.; Hashimoto, M.; Koshizuka, S.; Nishio, Y.; Moriya, H.; Yamazaki, M. Transplantation of bone marrow stromal cell-derived Schwann cells promotes axonal regeneration and functional recovery after complete transection of adult rat spinal cord. J. Neuropathol. Exp. Neurol. 64:37–45; 2005.

21. Keirstead, H. S.; Nistor, G.; Bernal, G.; Totoiu, M.; Cloutier, F.; Sharp, K.; Steward, O. Human embryonic stem cell-derived oligodendrocyte progenitor cell transplants remyelinate and restore locomotion after spinal cord injury. J. Neurosci. 25:4694–4705; 2005.
22. Kosacka, J.; Nowicki, M.; Kacza, J.; Borlak, J.; Engele, J.; Borowski, K. S. Adipocyte-derived angiopoietin-1 supports neurite outgrowth and synaptogenesis of sensory neurons. J. Neurosci. Res. 83:1160–1169; 2006.
23. Lee, I. H.; Bulte, J. W.; Schweinhardt, P.; Douglas, T.; Trifunovski, A.; Hofstetter, C.; Olson, L.; Spenger, C. In vivo magnetic resonance tracking of olfactory ensheathing glia grafted into the rat spinal cord. Exp. Neurol. 187:509–516; 2004.
24. Liang, H.; Liang, P.; Xu, Y.; Wu, J.; Liang, T.; Xu, X. DHAM-BMSC matrix promotes axonal regeneration and functional recovery after spinal cord injury in adult rats. J. Neurotrauma 26:1745–1757; 2009.
25. Lilja, J.; Endo, T.; Hofstetter, C.; Westman, E.; Young, J.; Olson, L.; Spenger, C. Blood oxygenation level-dependent visualization of synaptic relay stations of sensory pathways along the neuroaxis in response to graded sensory stimulation of a limb. J. Neurosci. 26:6330–6336; 2006.
26. Lu, J.; Feron, F.; Mackay-Sim, A.; Waite, P. M. Olfactory ensheathing cells promote locomotor recovery after delayed transplantation into transected spinal cord. Brain 125:14–21; 2002.
27. Ma, Y. H.; Zhang, Y.; Cao, L.; Su, J. C.; Wang, Z. W.; Xu, A. B.; Zhang, S. C. Effect of neurotrophin-3 genetically modified olfactory ensheathing cells transplantation on spinal cord injury. Cell Transplant. 19:167–177; 2010.
28. Matsuse, D.; Kitada, M.; Ogura, F.; Wakao, S.; Kohama, M.; Kira, J.; Tabata, Y.; Dezawa, M. Combined transplantation of bone marrow stromal cell-derived neural progenitor cells with a collagen sponge and basic fibroblast growth factor releasing microspheres enhances recovery after cerebral ischemia in rats. Tissue Eng. Part A 17:1993–2004; 2011.
29. Nguyen, T. H.; Khakhoulina, T.; Simmons, A.; Morel, P.; Trono, D. A simple and highly effective method for the stable transduction of uncultured porcine hepatocytes using lentiviral vector. Cell Transplant. 14:489–496; 2005.
30. Ogawa, S.; Menon, R. S.; Tank, D. W.; Kim, S. G.; Merkle, H.; Ellermann, J. M.; Ugurbil, K. Functional brain mapping by blood oxygenation level-dependent contrast magnetic resonance imaging. A comparison of signal characteristics with a biophysical model. Biophys. J. 64:803–812; 1993.
31. Okano, H.; Ogawa, Y.; Nakamura, M.; Kaneko, S.; Iwanami, A.; Toyama, Y. Transplantation of neural stem cells into the spinal cord after injury. Semin. Cell. Dev. Biol. 14:191–198; 2003.
32. Olson, L. Regeneration in the adult central nervous system: Experimental repair strategies. Nat. Med. 3:1329–1335; 1997.
33. Parr, A. M.; Kulbatski, I.; Tator, C. H. Transplantation of adult rat spinal cord stem/progenitor cells for spinal cord injury. J. Neurotrauma 24:835–845; 2007.
34. Parr, A. M.; Tator, C. H.; Keating, A. Bone marrow-derived mesenchymal stromal cells for the repair of central nervous system injury. Bone Marrow Transplant. 40:609–619; 2007.
35. Pawela, C. P.; Biswal, B. B.; Hudetz, A. G.; Li, R.; Jones, S. R.; Cho, Y. R.; Matloub, H. S.; Hyde, J. S. Interhemispheric neuroplasticity following limb deafferentation detected by resting-state functional connectivity magnetic resonance imaging (fcMRI) and functional magnetic resonance imaging (fMRI). Neuroimage 49:2467–2478; 2010.
36. Paxinos, G.; Watson, C. The rat brain in stereotaxic coordinates, the new coronal set, fifth ed. New York: Academic Press; 2005.
37. Sanganahalli, B. G.; Bailey, C. J.; Herman, P.; Hyder, F. Tactile and non-tactile sensory paradigms for fMRI and neurophysiologic studies in rodents. Methods. Mol. Biol. 489:213–242; 2009.
38. Schweinhardt, P.; Fransson, P.; Olson, L.; Spenger, C.; Andersson, J. L. A template for spatial normalisation of MR images of the rat brain. J. Neurosci. Methods 129:105–113; 2003.
39. Shimizu, S.; Kitada, M.; Ishikawa, H.; Itokazu, Y.; Wakao, S.; Dezawa, M. Peripheral nerve regeneration by the in vitro differentiated-human bone marrow stromal cells with Schwann cell property. Biochem. Biophys. Res. Commun. 359:915–920; 2007.
40. Spenger, C.; Josephson, A.; Klason, T.; Hoehn, M.; Schwindt, W.; Ingvar, M.; Olson, L. Functional MRI at 4.7 tesla of the rat brain during electric stimulation of forepaw, hindpaw, or tail in single- and multislice experiments. Exp. Neurol. 166:246–253; 2000.
41. Steward, O.; Sharp, K.; Selvan, G.; Hadden, A.; Hofstadter, M.; Au, E.; Roskams, J. A reassessment of the consequences of delayed transplantation of olfactory lamina propria following complete spinal cord transection in rats. Exp. Neurol. 198:483–499; 2006.
42. Sumiyoshi, A.; Riera, J. J.; Ogawa, T.; Kawashima, R. A mini-cap for simultaneous EEG and fMRI recording in rodents. Neuroimage 54:1951–1965; 2011.
43. von Bohlen Und Halbach, O. Immunohistological markers for staging neurogenesis in adult hippocampus. Cell Tissue Res. 329:409–420; 2007.
44. Wang, G.; Ao, Q.; Gong, K.; Zuo, H.; Gong, Y.; Zhang, X. Synergistic effect of neural stem cells and olfactory ensheathing cells on repair of adult rat spinal cord injury. Cell Transplant. 19:1325–1337; 2010.
45. Yiu, G.; He, Z. Glial inhibition of CNS axon regeneration. Nat. Rev. Neurosci. 7:617–627; 2006.

Isolation, culture and evaluation of multilineage-differentiating stress-enduring (Muse) cells

Yasumasa Kuroda[1,3], Shohei Wakao[2,3], Masaaki Kitada[2,3], Toru Murakami[2], Makoto Nojima[2] & Mari Dezawa[1,2]

[1]Department of Anatomy and Anthropology, Tohoku University Graduate School of Medicine, Sendai, Japan. [2]Department of Stem Cell Biology and Histology, Tohoku University Graduate School of Medicine, Sendai, Japan. [3]These authors contributed equally to this work. Correspondence should be addressed to Y.K. (y-kuroda@med.tohoku.ac.jp), M.K. (masaaki.kitada@gmail.com) or M.D. (mdezawa@med.tohoku.ac.jp).

Published online 20 June 2013; doi:10.1038/nprot.2013.076

Multilineage-differentiating stress-enduring (Muse) cells are distinct stem cells in mesenchymal cell populations with the capacity to self-renew, to differentiate into cells representative of all three germ layers from a single cell, and to repair damaged tissues by spontaneous differentiation into tissue-specific cells without forming teratomas. We describe step-by-step procedures for isolating and evaluating these cells. Muse cells are also a practical cell source for human induced pluripotent stem (iPS) cells with markedly high generation efficiency. They can be collected as cells that are double positive for stage-specific embryonic antigen-3 (SSEA-3) and CD105 from commercially available mesenchymal cells, such as adult human bone marrow stromal cells and dermal fibroblasts, or from fresh adult human bone marrow samples. Under both spontaneous and induced differentiation conditions, they show triploblastic differentiation. It takes 4–6 h to collect and 2 weeks to confirm the differentiation and self-renewal capacity of Muse cells.

INTRODUCTION

Mesenchymal stem cells (MSCs) are tissue stem cells that reside in mesenchymal tissues and that have attracted attention because of their unique properties. Generally, tissue stem cells are known to differentiate into the cell types of the tissue in which they reside; neural stem cells differentiate into neurons and glial cells, and hematopoietic stem cells give rise to all blood cell types[1,2]. Distinct from these tissue stem cells, MSCs have been reported to have the broad-ranged differentiation ability that crosses the oligolineage boundaries between the mesodermal and ectodermal or endodermal lineages[3,4]. In particular, the differentiation ability of bone marrow stromal cells (BMSCs), which are cultured as adherent cells from bone marrow aspirates, has been studied from the late 1990s up to the present time. BMSCs *in vitro* have been reported to give rise to cells not only in the same mesodermal lineage (osteocytes, chondrocytes, adipocytes[5,6], skeletal muscle cells[7–9], cardiac muscle cells[10,11] and endothelial cells[12,13]) but also in ectodermal (neuronal cells[14,15], Schwann cells[16,17]) and endodermal (hepatocytes[18,19], insulin-producing pancreatic beta cells[20,21]) lineages. In addition, when they are grafted into animals with tissue damage, BMSCs have been shown to spontaneously differentiate into and function as tissue-specific cells that replenish lost cells *in vivo*; therefore, BMSCs are presumed to act as the 'repairing cells'. This *in vivo* spontaneous differentiation has been demonstrated in skeletal muscle cells[22], cardiac muscle cells[23], neuronal cells[24], retinal cells[25], keratinocytes[26] and hepatocytes[27] after grafting, but as the efficiency of integration and differentiation is generally low, it is believed that only a particular subset of BMSCs can lead to such reparative effects. The similar differentiation abilities of mesenchymal cell populations have also been reported in adipose tissue[28], synovial tissue[29], dental pulp[30], umbilical cord[31] and dermis[32].

The above findings suggested that MSCs include a particular subset of stem cells that have the triploblastic differentiation ability that can give rise to various types of cells of all three germ layers and that can function as tissue-repairing cells *in vivo*. However, the 'stemness' of such cells has not been fully elucidated. The term 'MSCs' is generally used to represent cells that are collected from mesenchymal tissues by adherent culture, and therefore they are not composed of a single cell type but of crude heterogeneous cell populations. Classification as stem cells requires the presence of two fundamental properties: differentiation and self-renewal[33]. The triploblastic differentiation ability of MSCs mentioned above has largely been demonstrated by studies using crude heterogeneous MSCs, whose self-renewal property has not clearly been demonstrated[34,35]. Although there are some reports demonstrating the self-renewal property of a particular stem cell population of the MSCs, the differentiation ability presented in these studies was not triploblastic[36,37]. For these reasons, it has long been debated whether a specific stem cell population that shows both triploblastic differentiation and self-renewal capacity exists among MSCs[4,38].

Properties of Muse cells

Recently, we used a clonal analyis to identify a specific cell population that has a capacity for self-renewal and triploblastic differentiation similar to that of pluripotent stem cells in adult human mesenchymal cell populations[39]. We refer to this specific stem cell fraction as Muse cells because of their particular broad-ranged differentiation ability and stress tolerance. They can be collected as cells that are double-positive for the pluripotency marker SSEA-3 and the mesenchymal cell marker CD105 from commercially available mesenchymal cell populations, such as adult human BMSCs and dermal fibroblasts, or they can be collected from the mononuclear cell fraction of fresh adult human bone marrow aspirates. These cells express other pluripotency markers and have the property of self-renewal. A single Muse cell is able to give rise to not only mesodermal-lineage cells such as osteocytes, chondrocytes, adipocytes, smooth muscle cells and skeletal muscle cells but also ectodermal and endodermal cells such as neurons, epidermal cells, hepatocytes and biliary cells. Although these capacities of Muse cells are considered similar to those of other pluripotent stem cells, it is notable that, in contrast to embryonic stem (ES) cells or iPS cells, Muse cells are not immortal in culture or tumorigenic *in vivo*.

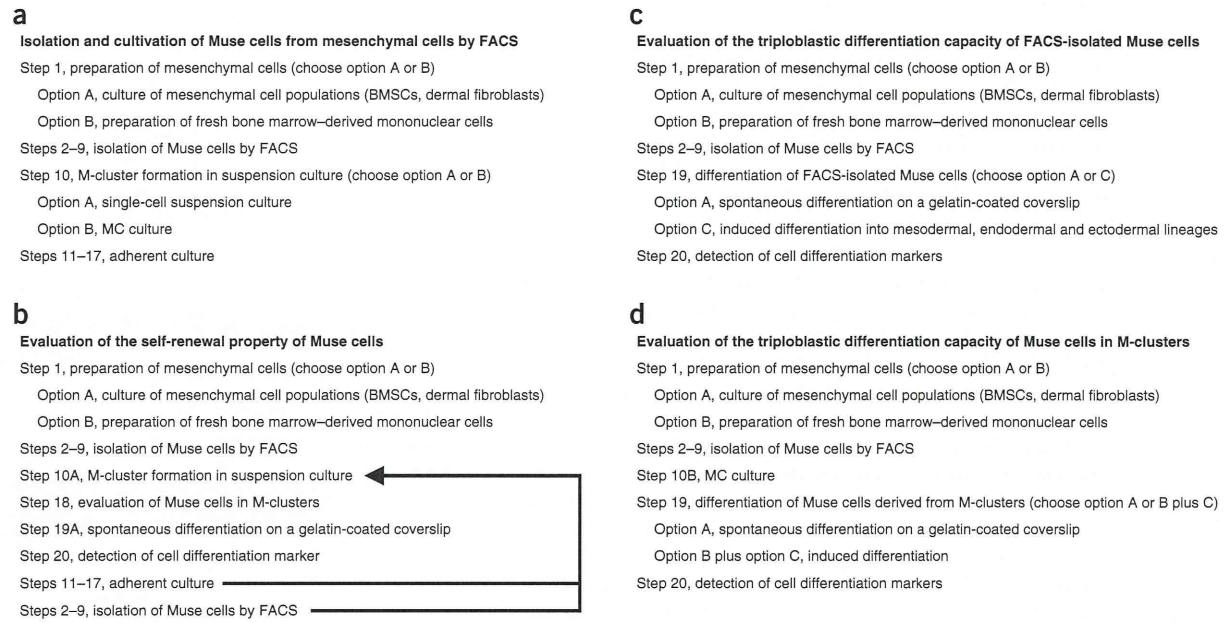

Figure 1 | Schematic overview of isolation, cultivation and evaluation of Muse cells.

Their telomerase activity is as low as that detected in adult dermal fibroblasts, and they do not form teratomas when transplanted into the testes of immunodeficient mice, as is often observed after transplantation of ES cells or iPS cells. *In vivo*, Muse cells can integrate into damaged tissues and spontaneously differentiate into tissue-specific marker–expressing cells according to the microenvironment when transplanted into animal models of fulminant hepatitis, skeletal muscle injury and skin injury[39]. Therefore, Muse cells are suggested to be the 'repairing cells' that have been postulated to exist among MSCs[39]. Another remarkable advantage of Muse cells is that they can be an efficient and practical cell source for iPS cell generation[40]. Adult human dermal fibroblast–derived Muse cells generated iPS cells with 30-fold higher efficiency than naive fibroblasts did, whereas cells other than Muse cells failed to form iPS cells, suggesting that Muse cells are virtually the original cell source for iPS cells among human dermal fibroblasts[40]. The unique capacities of Muse cells, including triploblastic differentiation, self-renewal, tissue repair without tumorigenic activity and high iPS cell–generation efficiency have great benefits not only in regenerative medicine but also in basic research into, for example, the full characterization of MSCs and the mechanisms of iPS cell generation.

Adult human mesenchymal tissues such as the bone marrow and dermis are known to contain several kinds of stem or progenitor cells such as multipotent adult progenitor cells, very small embryonic-like stem cells, marrow-isolated adult multilineage inducible cells, skin-derived precursors and $CD146^+$ osteoprogenitors[18,41–47], some of which are known to express pluripotency markers and are reported to have triploblastic differentiation ability similar to that of Muse cells[18,41–45]. However, the triploblastic differentiation ability of these stem cells has not been demonstrated at a single-cell level, as has been shown in Muse cells[40], so that pluripotentcy in the above-mentioned cell types has been, in the strict sense, an open question. The expression pattern of cell surface antigens in these stem cells is quite different from that in Muse cells, and, in particular, none of these stem cells express SSEA-3, by which Muse cells can be isolated directly from the adult mesenchymal tissue such as fresh bone marrow. Besides, when transplanted into the injured or degenerative tissues, Muse cells show high tissue-repairing activity, by which 80% or more Muse cells can differentiate into tissue-specific cell types, and they can replenish lost cells in damaged tissues[39]. A similarly high tissue-repairing activity has not been reported in the above-mentioned stem or progenitor cells. Thus, Muse cells are considered a distinct cell population from previously reported stem or progenitor cells among mesenchymal cell populations. Although some of the properties of Muse cells, namely self-renewal, triploblastic differentiation *in vitro* and tissue-repairing effect *in vivo*, have been clarified[39,40], future studies are required to elucidate the specific behavior of endogenous Muse cells, including the self-renewal property that has been demonstrated in a particular cell population of BMSCs[46,47], as well as their broad-ranged differentiation, the biological significance of the expression of pluripotency markers and the correlation between Muse cells and other tissue stem or progenitor cells.

Experimental design

We present here the protocol for isolation, cultivation and evaluation of Muse cells. A summary of our protocol is shown in **Figure 1**. We first describe the methods for preparation of mesenchymal cells (Step 1). In this section, the detailed protocol for culturing BMSCs and dermal fibroblasts is described (Step 1A), because the viability and isolation efficiency of Muse cells are highly dependent on the basic culture method of these mesenchymal cells. As Muse cells can be isolated from mononuclear cells from fresh bone marrow, the protocol for preparing